Correlated Magnetic Vortex Chains in Mesoscopic Cobalt Dot Arrays

M. Natali,[1] I. L. Prejbeanu,[2] A. Lebib,[1] L. D. Buda,[2] K. Ounadjela,[2] and Y. Chen[1,*]
[1]*Laboratoire de Photonique et Nanostructures LPN-CNRS, Route de Nozay, 91460 Marcoussis, France*
[2]*Institut de Physique et Chimie des Matériaux de Strasbourg, IPCMS (UMR 7504 CNRS-ULP) 23 rue du Loess, 67037 Strasbourg, France*
(Received 28 June 2001; published 1 April 2002)

Nucleation and annihilation of vortex states have been studied in two-dimensional arrays of densely packed cobalt dots. A clear signature of dipolar interactions both between single-domain state dots and vortex state dots has been observed from the dependence of vortex nucleation and annihilation fields on interdot separation. A direct consequence of these interactions is the formation of vortex chains as well as dipole chains aligned along the direction of the external field. In addition, short range correlation of chiralities within vortex chains has been observed using magnetic force microscopy imaging and has been attributed to cross-talking between adjacent elements.

DOI: 10.1103/PhysRevLett.88.157203 PACS numbers: 75.60.–d, 68.37.Rt, 75.75.+a, 78.20.Ls

One of the challenges in the development of high density magnetic data storage media and magnetoresistive memory chips is reducing the cross-talk between adjacent magnetic elements. It is known that dipolar interactions between single domain magnetic elements introduce a distribution of switching fields which may lead to nonreproducible switching of the bits [1–3]. Recently, stable magnetic vortices that form in ferromagnetic dots [4,5] and rings [6–8], have attracted much attention in view of the possibility of reducing magnetostatic interactions. Compared to single domain states, magnetic vortices have a much lower stray field, due to the flux closure configuration, and may thus be packed more densely.

Besides the technological application, magnetic vortices in patterned magnetic elements are of interest also from a basic physics point of view. The vortex nucleation and annihilation mechanism has been mainly investigated for widely spaced dots, both theoretically and experimentally [4,5,9,10]. However, not many studies analyzed how this mechanism is altered in the case of arrays of densely packed dots [11].

In this Letter we investigate the effect of dipolar interactions on the magnetization configuration of densely packed circular Co dots. Experimental observations by magnetic force microscopy (MFM) and magneto-optic Kerr effect (MOKE), together with numerical simulations, have shown that the nucleation of vortices in densely packed arrays is correlated for neighboring dots, forming vortex chains, with a direct consequence on their chirality.

Arrays of 30 nm thick polycrystalline circular Co dots were fabricated by nanoimprint lithography and lift-off technique [12]. The dots are arranged in a 150 × 150 μm^2 area and disposed in a square lattice. For dots with diameters (ϕ) 550 and 1000 nm, the interdot separation (S), defined as the distance between the dot centers, was varied yielding arrays with the following spacing/diameter ratios S/ϕ: 1.1, 1.5, 2, and 3. The MOKE hysteresis loops, recorded with a 10 μm focal spot, were measured in longitudinal geometry at room temperature. The MFM measurements were performed in the phase detection mode (Nanoscope Dimension 3100) using commercial CoCr coated Si cantilever tips of pyramidal shape magnetized along the tip axis. The magnetic configurations were imaged at a lift height of 100 nm and an in-plane external magnetic field was applied during the image acquisition.

The MOKE hysteresis loop obtained for an array of Co dots with $\phi/S = 550/1500$ nm is shown in Fig. 1(a). For large negative values of the external field, the dots adopt

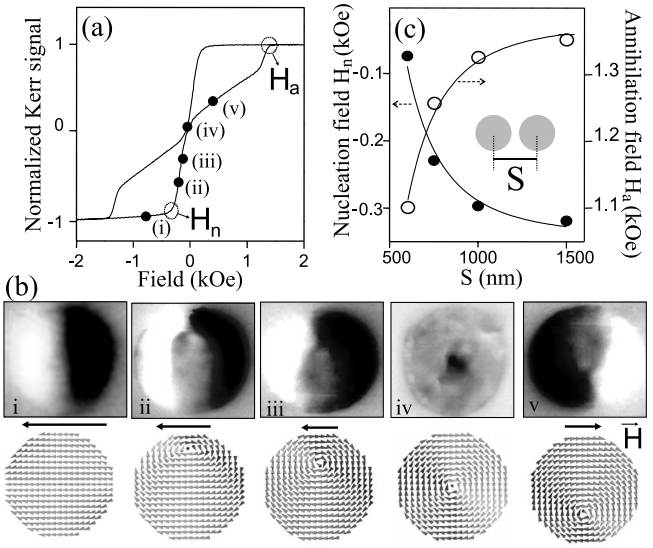

FIG. 1. (a) Longitudinal MOKE hysteresis loop of a $\phi/S = 550/1500$ nm Co dot array. (b) MFM images of typical micromagnetic configurations along the hysteresis loop in dots with $\phi = 1000$ nm: (i) SD state in negative field, (ii),(iii) distorted vortex states in negative field, (iv) vortex state in zero field, (v) displaced vortex state in positive field. In the bottom of each image, the corresponding simulated magnetization distributions are shown. For clarity the arrows represent only a subset of the cells in the calculation. (c) Vortex nucleation and annihilation fields as a function of interdot separation, for $\phi = 550$ nm.

an in-plane single domain (SD) configuration [Fig. 1(b)-i], with a characteristic black and white MFM contrast. Starting from this configuration and increasing the field towards positive values, the magnetization value drops at the nucleation field H_n, when a vortex nucleates at the dot border [Fig. 1(b)-ii]. By further increasing the field, the vortex moves towards the dot center [Fig. 1(b)-iii] and a completely symmetric configuration is stabilized at zero field [Fig. 1(b)-iv]. In this particular state, the circular flux closure of the magnetization does not produce any substantial lateral magnetic stray field, and the only contrast arises from the vortex core located at the dot center. Upon increasing the field, the net magnetization progressively reappears as the vortex moves towards the opposite dot border, giving rise to a dipolar contrast which gradually develops [Fig. 1(b)-v]. Finally, above the annihilation field H_a, the vortex is expelled from the dot and a single domain state is again established. The evolution of the internal structure of the magnetization is illustrated clearly by the simulated configurations [13]. For a given orientation of the applied field, the vortex core moves either up or down, depending on the clockwise or counterclockwise circulation of the flux. This defines the chirality of the vortex and it is found to be easily identified from the MFM images for dot sizes above 500 nm. For smaller dot diameters, the MFM contrast did not allow identification of the chirality of the vortex, the contrast of the displaced vortex being indistinguishable from SD magnetic contrast.

The influence of the dipolar interactions is reflected in both the nucleation and annihilation field's behavior. Their variation with the interdot separation, for an array of dots with $\phi = 550$ nm, is illustrated in Fig. 1(c) and is compatible with a significant increase of the interaction fields for spacing below 1000 nm. The experimental data are well fitted by the expression $H_{n/a} = H_{n/a}(\infty) \pm 4.2 M_s (V/S^3)$ that describes the interaction field in a two-dimensional square lattice of dipoles [14]. Here V denotes the volume of the dot and M_s is the saturation magnetization of Co (1400 emu/cm^3). The fitting parameter used, $H_{n/a}(\infty)$, represents the nucleation/annihilation field for isolated dots. The right-hand side term gives the dipolar interaction field which acts at nucleation (+) and annihilation (−). As underlined before, the vortex states are not expected to interact due to the flux closure configuration. However, this is true only for vortices which are completely symmetric with respect to the center of the dot. In contrast, just below H_a, the vortex states are strongly distorted. The analogous behavior of the fitting curves for annihilation/nucleation [Fig. 1(c)] indicates that the effective dipole moment existing before annihilation is almost identical with that of a SD dot.

The interaction among the dots has been further investigated using MFM. For the case of a dense array [Fig. 2(a)], upon increasing the field from negative saturation, the vortices nucleate along chains aligned parallel to the applied field direction. The first chains appear at about −300 Oe [Fig. 2(a)-i]. No vortices were observed at −325 Oe. The

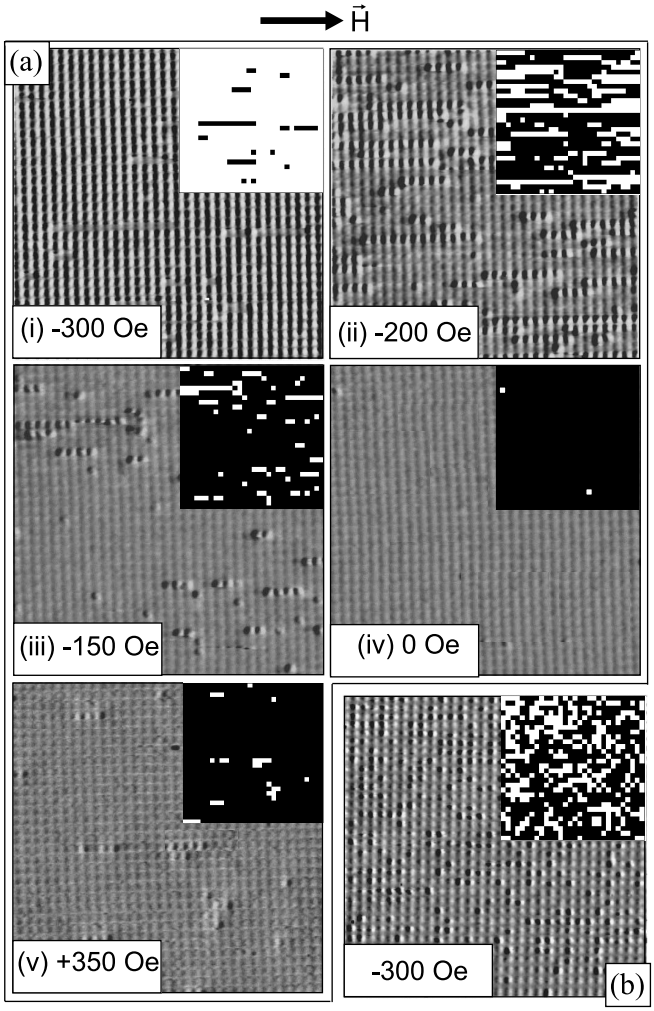

FIG. 2. MFM images showing the distribution of SD and vortex states. The inset of each figure shows graphic elaborations of the MFM images and represents vortices as black squares and SD states as white squares. (a) Array of strongly interacting dots with $\phi/S = 550/600$ nm (scan size 20×20 μm^2). The magnetic field is increased from negative saturation (−1.5 kOe) to zero (i)–(iv). Starting from the situation (iv), the field is increased to +1 kOe and then decreased to +350 Oe (v). (b) Array of widely spaced dots with $\phi/S = 550/1000$ nm (scan size 32×32 μm^2). The magnetic history is the same as for (a)-(i).

number and length of chains increase by further increasing the field until almost all dots are in the vortex state [Fig. 2(a-ii)–2(a-iv)]. The formation of the vortex chains may be understood as follows: when a dot in a SD state transforms into a vortex state, adjacent dots, lying on the same line parallel to the applied field, experience a lower effective magnetic field than the other dots, due to the loss of dipolar coupling. As a consequence, the adjacent dots prefer to switch to the vortex state. By repeating this process, vortex chains form along the field direction. To stress that the chain formation is not induced by the MFM tip-sample interaction, scans taken at 90° with respect to the external field reveal that the chains still remain oriented along the direction of the field.

In contrast, for widely spaced dots [Fig. 2(b)] for which the interactions are drastically reduced, the vortices nucleate almost randomly. Moreover, the number of vortices, compared to the denser array for the same applied field (-300 Oe) [Fig. 2(a)-i], is larger by 1 order of magnitude. This indicates that the SD state is stabilized by the interaction fields and that the chain formation observed in densely packed arrays is a clear signature of dipolar interactions.

To investigate the effect of interactions on the annihilation process, the field was first increased up to $+1$ kOe, slightly below the measured annihilation field extracted from the MOKE measurements. A finite number of SD states are generated at this field because of the annihilation field distribution. Then, to better visualize the SD states, we decrease the field to $+350$ Oe and record the MFM image shown in Fig. 2(a)-v. Chains of SD dots parallel to the applied field are observed. This effect is once again a clear signature of the additional energetic contribution of the dipolar interaction to the neighboring dots.

A short range correlation between the chiralities of neighboring dots has been evidenced in an array of interacting dots. Relatively long chains of vortices having the same chirality (up to 7 dots) along the field direction have been observed such as those shown in Fig. 3(a). The chirality of the vortices is indicated using arrows rotating clockwise or counterclockwise. The average length of the chains with the same chirality, obtained using several scans, is around 3 dots. In contrast, the average length measured on a widely spaced array of dots is about 2 dots and corresponds to the calculated length of a random distribution of the chirality of vortices [15]. We also observe that when approaching the vortex nucleation field, the magnetization of the SD state starts to deviate from the applied field direction and a correlated tilt of the effective dipole moments develops resulting in a characteristic zigzag configuration, shown in Fig. 3(b).

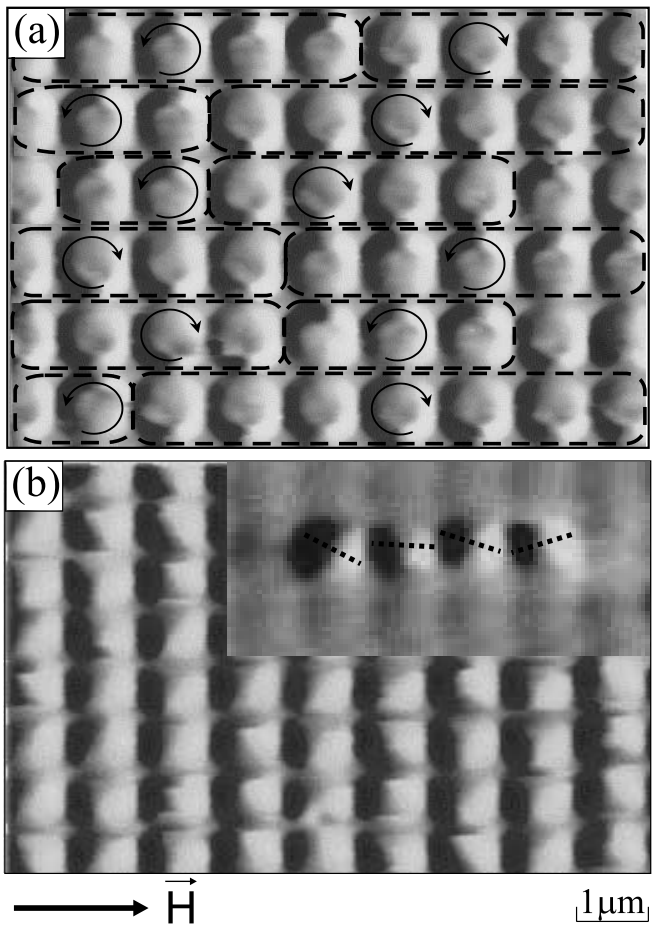

FIG. 3. (a) MFM image of a $\phi/S = 1000/1100$ nm array of displaced vortices in a 250 Oe field, showing the distribution of the chains of vortices with the same chirality. (b) MFM images of SD states close to vortex nucleation in arrays $\phi/S = 1000/1100$ nm and $\phi/S = 550/600$ nm in the inset.

To clarify the physical origin of the zigzag configuration and the correlation of vortex chiralities micromagnetic simulations were performed [13]. In Fig. 4, results are reported for a chain of 7 dots with 170 nm dot diameter, 200 nm period and 30 nm dot thickness. This is the largest system size compatible with the available computing resources, given that the mesh size needs to be smaller than the exchange length of cobalt (4 nm). The chain is first saturated in a large negative field, applied along its axis, and then the field is increased towards positive values in steps of 10 Oe.

The equilibrium configuration for a chain with fixed boundary conditions at both ends [16] is shown in Fig. 4(a) at an applied field of $+200$ Oe. A zigzag configuration is obtained, similar to that in the MFM images [Fig. 3(b)]. The simulations also show an inhomogeneous magnetization distribution inside the dots, known as "magnetization buckling." The development of a zigzag configuration originates from the attraction of opposite magnetic charges on adjacent dots. To mimic the effect of a distribution of vortex nucleation fields, the boundary condition at the left end is relaxed [Fig. 4(b)]. This allows initiation of the nucleation process in dot-1 at $+30$ Oe coming from negative saturation. By increasing the field, a nucleation avalanche is triggered and vortices nucleate successively in dot-2, dot-3, etc. until all dots are in the vortex state at equilibrium. Interestingly all the nucleated vortices have the same chirality, imposed by the first vortex.

The origin of the chirality correlation can be understood in terms of magnetostatic interactions as follows: during the magnetization buckling that accompanies vortex formation, the surface charges of the SD state approach each other moving along the dot border. The charges annihilate where the vortex core enters the dot, this location determining the vortex chirality [see discussion of Fig. 1(b)]. The interaction of magnetic charges on adjacent dots induces a correlation in the charge movement and thereby imposes the location of vortex nucleation which in turn determines the vortex chirality. Simulations on chains with different dot diameters have shown that a correlation of vortex chiralities occurs also for dots with larger ($\phi = 400$ nm) and smaller ($\phi = 60$ nm) diameters. In all cases the origin of the correlations is related to magnetostatic coupling

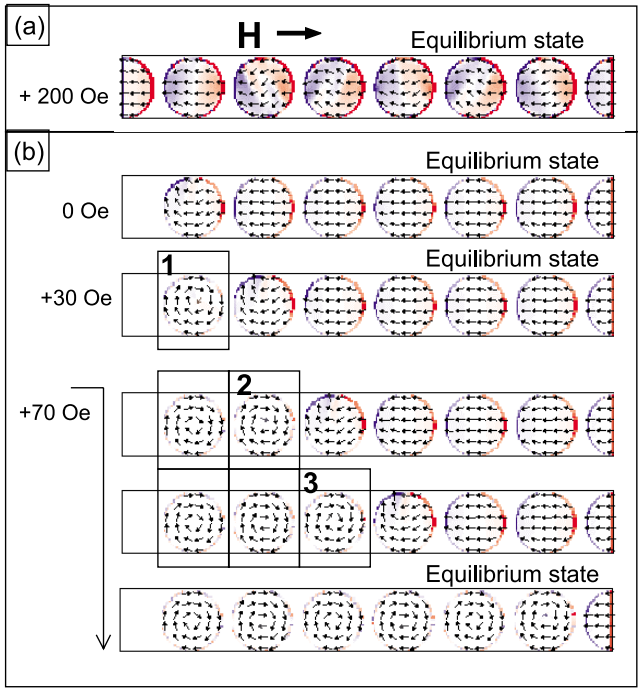

FIG. 4 (color). Micromagnetic simulation of vortex nucleation process in a chain of magnetostatically coupled Co dots ($\phi/S = 170/200$ nm, thickness 30 nm). Magnetic charges are represented by a blue/red color code: blue for positive and red for negative magnetic charges. (a) Zigzag configuration determined by correlated magnetization buckling. (b) Formation of a chain of vortices with identical chirality. The scale of the color code is reduced by a factor of 3 in (b) compared to (a) to highlight surface charges.

between adjacent dots. Based on the scaling of the dipolar interaction field with dot diameter at constant ϕ/S ratio we conclude that the energy involved in the interactions, that determines the correlations, increases with decreasing dot size, underlining the possible implication for ultrahigh density storage.

Concerning the comparison with our experimental results on dots with diameter $\phi = 1$ μm, the short correlation length ($N = 3$ dots) probably is a consequence of the relatively weak interaction field on these dots (100 Oe compared to 500 Oe, in Fig. 4). Moreover, in the real samples the distribution of vortex nucleation fields may lead to nucleation of two or more independent vortices in the same row in non adjacent dots with opposite chirality, generating frustration within the row.

In conclusion, the mechanism of vortex nucleation/annihilation in arrays of densely packed cobalt dots is influenced by the magnetostatic coupling between the dots. The vortex nucleation and annihilation fields follow a spacing dependence which can be described in terms of dipolar interaction between uniformly magnetized dots. Chains of vortices with correlated chiralities have been observed as well as chains of single-domain dots formed during vortex annihilation. Micromagnetic simulations identify the origin of the correlations in the magnetostatic coupling between adjacent dots.

The authors gratefully acknowledge L. Couraud for technical support and U. Ebels for useful discussions. This work was partially supported by EC No. FMRX-CT97-0147 "SUBMAGDEV" and by EC No. HPRN-CT-1999-00150 "NANOSCALE PARTICLES."

*Email address: yong.chen@lpn.cnrs.fr

[1] T. Aign, P. Meyer, S. Lemerle, J. P. Jamet, J. Ferré, V. Mathet, C. Chappert, J. Gierak, C. Vieu, F. Rousseaux, H. Launois, and H. Bernas, Phys. Rev. Lett. **81**, 5656 (1998).

[2] G. A. Gibson and S. Schultz, J. Appl. Phys. **73**, 4516 (1993).

[3] R. Proksch and B. Moskowitz, J. Appl. Phys. **75**, 5894 (1994).

[4] R. P. Cowburn, D. K. Koltsov, A. O. Adeyeye, M. E. Welland, and D. M. Tricker, Phys. Rev. Lett. **83**, 1042 (1999).

[5] A. Lebib, S. P. Li, M. Natali, and Y. Chen, J. Appl. Phys. **89**, 3892 (2001).

[6] S. P. Li, D. Peyrade, M. Natali, A. Lebib, Y. Chen, U. Ebels, L. D. Buda, and K. Ounadjela, Phys. Rev. Lett. **86**, 1102 (2001).

[7] J. Rothman, M. Kläui, L. Lopez-Diaz, C. A. F. Vaz, A. Bleloch, J. A. C. Bland, Z. Cui, and R. Speaks, Phys. Rev. Lett. **86**, 1098 (2001).

[8] K. Bussmann, G. A. Prinz, R. Brass, and J. G. Zhu, Appl. Phys. Lett. **78**, 2029 (2001).

[9] A. Fernandez and C. J. Cerjan, J. Appl. Phys. **87**, 1395 (2000).

[10] M. Schneider, H. Hoffmann, and J. Zweck, Appl. Phys. Lett. **77**, 2909 (2000).

[11] R. E. Dunin-Borkowsky, M. R. McCartney, B. Kardinal, D. J. Smith, and M. R. Scheinfein, Appl. Phys. Lett. **75**, 2641 (1999).

[12] A. Lebib, Y. Chen, F. Carcenac, E. Cambril, L. Manin, L. Couraud, and H. Launois, Microelectron. Eng. **53**, 175 (2000).

[13] http://math.nist.gov/oommf/ The micromagnetic OOMMF code provides the stable magnetic states of a ferromagnetic system following an energy minimization procedure based on the Landau-Lifshitz-Gilbert equation time integration. All the simulations reported here were tested using different mesh size and no significant modifications of the magnetic behavior were found if the mesh size used is below the exchange length of cobalt.

[14] M. Grimsditch, Y. Jaccard, and I. K. Schuller, Phys. Rev. B **58**, 11 539 (1998).

[15] For a random distribution the two possible vortex chiralities appear with equal probability, 1/2. The probability to find N independent vortices with the same chirality is $(1/2)^N$.

[16] To simulate the behavior of an infinite chain (i) we fix the magnetization of the half-dots at the left and right end of the chain in the SD state; (ii) we add constant charge distributions of magnitude $+/-M_s\pi(\phi/2S)^2$ at the left/right end of the chain, respectively, to compensate for the demagnetization field that arises because of the finite system size.